The importance of the cathode plume and its interactions with the ion beam in numerical simulations of Hall thrusters

IEPC-2015-310／ISTS-2015-b-310

Presented at Joint Conference of 30th International Symposium on Space Technology and Science 34th International Electric Propulsion Conference and 6th Nano-satellite Symposium, Hyogo-Kobe, Japan July 4 – 10, 2015

Alejandro Lopez Ortega[1] and Ioannis G. Mikellides[2]
Jet Propulsion Laboratory, California Institute of Technology, Pasadena, CA, 91109, United States

Abstract: Hall2De is a first-principles, 2-D axisymmetric code that solves the equations of motion for ions, electrons, and neutrals on a magnetic-field-aligned grid. The computational domain downstream of the acceleration channel exit plane is large enough to include self-consistently the cathode boundary. In this paper, we present results from numerical simulations of the H6 laboratory thruster with an internally mounted cathode, with the aim of highlighting the importance of properly accounting for the interactions between the ion beam and cathode plume. The anomalous transport of electrons across magnetic field lines in Hall2De is modelled using an anomalous collision frequency, ν_{anom}, yielding $\nu_{anom}\approx\omega_{ce}$ (i.e., the electron cyclotron frequency) in the plume. We first show that restricting the anomalous collision frequency to only regions where the current density of ions is large does not alter the plasma discharge in the Hall thruster as long as the interaction between the ion beam and the cathode plume is captured properly in the computational domain. This implies that the boundary conditions must be placed sufficiently far as to not interfere with the electron transport in this region. These simulation results suggest that electron transport across magnetic field lines occurs largely inside the beam and may be driven by the interactions between beam ions and electrons. A second finding that puts in relevance the importance of including the cathode plume in numerical simulations is on the significance of accounting for the ion acoustic turbulence (IAT), now known to occur in the vicinity of the cathode exit. We have included in the Hall2De simulations a model of the IAT-driven anomalous collision frequency based on Sagdeev's model for saturation of the ion-acoustic instability. This implementation has allowed us to achieve excellent agreement with experimental measurements in the near plume obtained during the operation of the H6 thruster at nominal conditions (300V, 20A) and chamber background pressure of approximately $1.5\text{x}10^{-5}$ Torr. In addition, the numerical results obtained with the latter approach exhibit less sensitivity to background pressure than previous attempts at explaining the features of the plasma properties in the near plume.

Nomenclature

$\mathbf{B}$	=	magnetic field vector
$\boldsymbol{\beta}$	=	unitary vector in the direction of the magnetic field
$\mathbf{E}$	=	electric field vector
ε_0	=	vacuum permittivity
η	=	electrical resistivity

[1] Member of the Technical Staff, Electric Propulsion group, alejandro.lopez.ortega@jpl.nasa.gov.
[2] Principal Engineer, Electric Propulsion group, ioannis.g.mikellides@jpl.nasa.gov.

η_{ei}	=	equivalent resistivity due to ion current
$\mathbf{j}$	=	current density
J	=	current (modulus)
K	=	coefficient in cathode anomalous collision frequency model
L	=	length of acceleration channel
m	=	particle mass
n	=	number density
Ω	=	Hall parameter
p	=	pressure
ϕ	=	plasma potential
q	=	particle charge
r	=	radial coordinate
$R_{midchannel}$	=	distance between the channel centerline and thruster centerline
T	=	temperature (in electron-volts, eV)
u	=	velocity modulus
$\mathbf{u}$	=	drift velocity vector
ν	=	collision frequency
z	=	axial coordinate
anom	=	(subscript) anomalous
e	=	(subscript) electron property
eGyro	=	(subscript) electron-cyclotron
ei	=	(subscript) electron-ion
en	=	(subscript) electron-neutral
i	=	(subscript) ion property

I. Introduction

Modeling and simulation activities of the plasma discharge in Hall-effect thrusters (HET) play an important role in investigating the physical principles behind the operation of these devices. Numerical methods are also useful tools for guiding the design of HETs due to their versatility at the time of rapidly modifying physical parameters, geometry, or operating conditions.

One common approach for simulating the plasma conditions in Hall thrusters makes use of a hydrodynamic ("fluid") formulation for modeling the motion of electrons. The zeroth, first, and second moments of Boltzmann's evolution equation for the electron distribution function are integrated over velocity space, resulting in an equation for mass conservation, three equations for tracking the evolution of the average velocity field, and one energy equation. Due to the low mass of the electrons, the inertia terms are commonly neglected in the momentum equation, the resultant expression being then equivalent to the vector form of Ohm's law. The transport coefficients that appear in Ohm's law, such as the resistivity, are determined under the assumption that the electrons follow a Maxwellian distribution. This approach has advantages over particle-in-cell (PIC) methods [1-3] (in which a set of hyper-particles representing the electrons move in the computational domain according to Lorentz's force) in the sense that fluid algorithms produce low levels of noise in the solution, combined with a moderate computational cost that allow them to be run in workstation-class computers. The most widely adopted among the algorithms that use a hydrodynamic formulation for electrons is HPHall [4] (afterwards upgraded to HPHall(2) [5]), which earned the distinction of being the first two-dimensional algorithm to reproduce breathing mode oscillations [6-8] in Hall thrusters. HPHall takes advantage of the high values of the Hall parameter Ω_e (i.e., the ratio of the cyclotron frequency of electrons in a magnetic field and the collision frequency) for decoupling the motion of electrons in the directions parallel and perpendicular to magnetic field lines. Since resistivity across magnetic field lines (B-lines) is much higher (by an order of Ω_e^2) than along them, HPHall solves Ohm's law in the direction perpendicular to the magnetic field whilst electron temperature is considered isothermal and Boltzmann's relation for electrons is applied along B-lines. Hall2De [9], which has been developed at the Jet Propulsion Laboratory for the past decade and is the subject matter of this article, solves Ohm's law without making any assumption on force lines being also isothermal lines. Early Hall2De simulations showed that while isothermality along magnetic field lines is indeed maintained inside the thruster channel and the near plume, isothermal lines do not follow this pattern in the cathode plume.

Despite the computational advantages of hydrodynamics codes, the implementation of a numerical algorithm fully reliant on physical first-principles has not been possible to date. The reason for this is that classical collision theory predicts resistivity values across magnetic field lines that are much larger than those required for reproducing the plasma measurements reported in experiments. Since the cause of this enhanced collisionality remains uncertain, numerical and analytical studies have historically accounted for this phenomenon by including an anomalous collision frequency term in the computation of transport coefficients that effectively reduces the Hall parameter. In the original HPHall simulations [4], the anomalous term was taken proportional to the magnitude of the magnetic field using Bohm's scaling [10]. The implementation followed in Hall2De consists of the cyclotron frequency multiplied by a profile that changes along the centerline of the acceleration channel and is extended two-dimensionally along magnetic field lines [11]. This profile has been improved as new experimental measurements have become available. The aim of this approach is to accurately capture the plasma properties reported in experiments and then try to gain physical insight on the mechanism driving the reduced resistivity by identifying the amount of anomalous collision frequency required in the Hall thruster and its near plume. A first attempt at implementing a self-consistent model for the anomalous collision frequency in Hall2De is presented in our companion paper [12]. The model implemented there is based on the hypothesis that the enhanced electron transport is caused by the electron cyclotron drift instability [13], which has maximum growth in the acceleration region of the Hall thruster and is convected to the plume by the thruster main beam. Numerical simulations using PIC algorithms [2,14], and a combination of analysis and measurements [15-17] suggest that this hypothesis constitutes a sensible statement for explaining the presence of anomalous transport in Hall thruster plumes.

Another region in which the classical transport of electrons is modified by collisionless mechanisms is the cathode plume. Extensive evidence of this phenomenon was found on a decade-long experimental and numerical effort at the Jet Propulsion Laboratory to understand the plasma conditions downstream of the keeper exit in hollow cathodes used for electric propulsion [18-21]. The conclusions, which have been recently extended to cathodes operating at discharge currents in the vicinity of 100A [22-24], indicate that plasma conditions conducive to the excitement of ion-acoustic turbulence (IAT) occur downstream of the keeper exit. Hall2De was the first numerical code used in Hall thruster simulations to incorporate the real physical location of the cathode instead of a fictitious cathode modeled as a boundary condition that acts as a source of electron current. However, in previous iterations of the code, a model for the presence of anomalous collision frequency in the cathode plume had not been implemented.

The objective of this paper is to highlight a series of improvements made over the past year in the Hall2De algorithm towards our goal to produce self-consistent plasma simulations that could explain accurately the plasma features observed in experimental measurements. In particular, we focus on understanding the motion of electrons from their source in the cathode to the acceleration channel and how the interaction between the cathode plume and the ion beam plays a role in this transport. Section II contains a general description of the current version of the Hall2De algorithm. In Section III, we emphasize the importance for our investigations of employing a computational domain with the appropriate dimensions such that the boundary conditions do not alter the transport of electrons across magnetic field lines. Section IV shows that the anomalous collision frequency necessary to transport electrons towards the thruster channel can be neglected in regions of low ion density, without changes in the performance or the plasma properties. This result partially motivated the hypothesis described in [12], which postulates that the instabilities generated in the acceleration channel can be transported by the stream of beam ions into the plume. In Section V, we discuss the effect of including a simple model for the anomalous collision frequency in the cathode plume. Section VI summarizes the most important findings of this investigation.

II. Computational method

A typical computational domain in Hall2De is depicted in Fig. 1. In the acceleration channel, the flow of neutral particles injected at the anode is ionized by electron impacts. In the acceleration region, the ions are accelerated due to the potential gradient caused by the large resistivity to the electron transport across magnetic field lines. Downstream of this location, the ion beam expands into the plume region. Fig. 1 shows a configuration with a centrally mounted cathode. The exact location of the cathode is replicated in the computational domain and the cathode plume included self-consistently in the simulations. This computational domain is discretized making use of a quadrilateral magnetic-field-aligned mesh (MFAM) [25,26] with edges parallel and perpendicular to the magnetic field lines.

The motion of neutral species in Hall2De is modeled as free molecular flow and numerically implemented using the algorithm described in [27]. Neutrals are considered to describe straight paths from the surfaces they originate. The boundaries of the computational domain are modeled as emissive, receptive, or reflective surfaces and view-factors of each of the boundaries with respect to one another are computed. These view-factors are used for determining the fraction of neutrals that cross each of the boundaries and to reconstruct the density and velocity fields of atoms. Loss of neutral atoms due to ionization is included through a mass conservation statement.

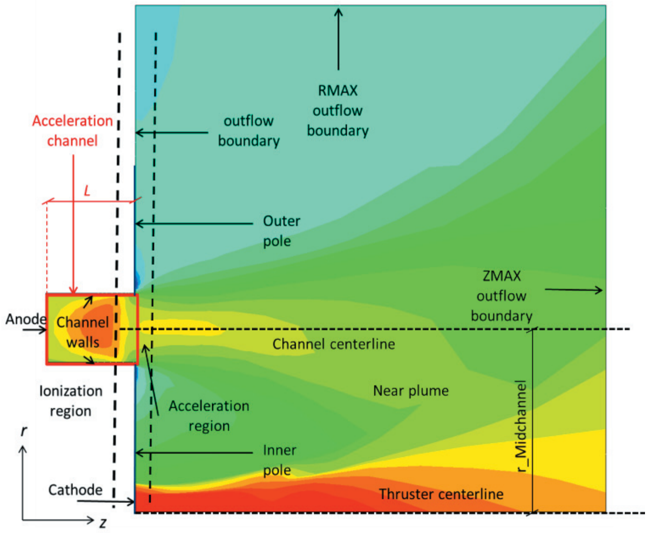

Fig. 1: Hall2De computational domain of the H6 lab thruster [28,29] showing naming conventions for the different thruster elements and plasma regions.

Hall2De employs a hydrodynamic formulation for modeling the motion of ions in the computational domain. This approach contrasts with discrete particle methodologies (for instance, followed in HPHall [4]) where ions are modeled as hyper-particles in a PIC algorithm, owing to their low collisionality. However, it was shown in [9] that ion-ion collisions in the ionization region are sufficient (under typical plasma conditions) to warrant a hydrodynamic description of the ionized particles. In the acceleration region, the ion motion is mainly driven by the large voltage differential, which can accelerate ions to velocities that exceed 20 km/s. Under these plasma conditions, the motion of ions is driven by the equilibrium between the inertial terms and the acceleration due to the electric field and the equations of motion in the PIC and fluid approaches become similar. In the plume region, two populations of ions exist: the main beam of high-energy ions and a secondary population of slower ions that originate at the cathode, or due to charge exchange and ionization downstream of the steep potential gradient. Beam ions do not undergo considerable collisions due to their large velocities but as their residence time is small, deviations from an equilibrium distribution are not likely to occur. The low-energy particles undergo sufficient collisions between them in most of the near plume region to justify a hydrodynamic modeling approach but do not interact sufficiently with the beam ions (due to their high relative drift velocity) to warrant the existence of a single ion population. For typical values of beam ion density ~$5\text{x}10^{17}$ m^{-3} and drift velocity ~16000 m/s, the collision time between high and low energy ions is ~$4\text{x}10^{-3}$ s, compared to a typical residence time in the computational domain for low-energy particles of ~$5\text{x}10^{-5}$ s. In Hall2De, we allow for different ion populations in the plume by making use of a multi-fluid algorithm that overcomes the difficulties that single-fluid simulations encounter in the near plume (namely an under-estimation of the plasma density), while eliminating statistical noise typical of PIC formulations. A description of the equations of motion for ions and their implementation in the multi-fluid approach can be found in [30]

The plasma density and temperature are obtained from the quasi-neutrality assumption and the solution of the electron energy equation, respectively. A closure for the system of equations that allows for the complete determination of the plasma properties is provided by combining the current conservation statement with the vector form of Ohm's law,

$$\mathbf{E} = \eta \mathbf{j}_e + \eta \Omega_e \mathbf{j}_e \times \boldsymbol{\beta} - \frac{\nabla p_e}{q_e n_e} + \eta_{ei} \mathbf{j}_i, \tag{1}$$

with $\Omega_e = |\mathbf{B}| / (q n_e \eta)$ the Hall parameter for electrons. The resistivity is defined as

$$\eta = \frac{m_e (\nu_{ei} + \nu_{en} + \nu_{anom})}{q_e^2 n_e}, \tag{2}$$

where ν_{ei} and ν_{en} are the averaged electron-ion and electron-neutral collision frequencies. ν_{anom} is the anomalous collision frequency, added to account for the non-classical transport that has been found to persist in Hall thrusters. Two mechanisms of anomalous electron transport are considered in the computational domain. Along the main beam of ions, anomalous transport only exists in the direction perpendicular to the magnetic field lines and is modeled using values that have been determined based on comparisons with experimental measurements [11]. In the cathode plume region, anomalous transport occurs as a consequence of the ion-acoustic instability and it is modeled using Sagdeev's expression for the wave saturation [31],

$$\nu_{anom,cath} = K\sqrt{\frac{n_e q_e^2}{m_i \varepsilon_0}}\frac{|\mathbf{u}_e|}{c_e}, c_e = \sqrt{\frac{2q_e T_e}{m_e}}, \tag{3}$$

where K is a parameter than needs to be determined based on comparisons with plasma measurements. This source of anomalous transport is considered to act isotropically in all directions. Its effect is however mostly in the parallel direction as the electron current essentially parallels magnetic field lines in the cathode plume.

III. The importance of the near-plume computational domain

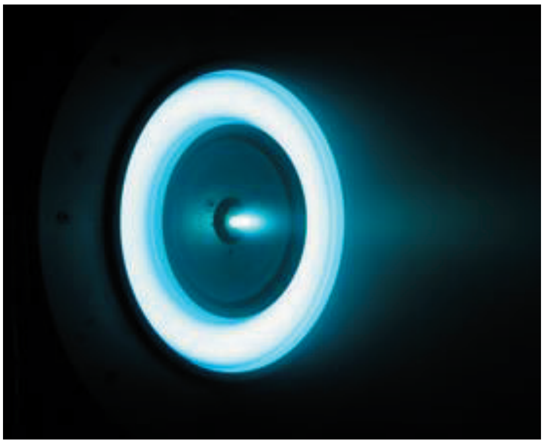

Fig. 3: H6 laboratory thruster in operation

The numerical simulations reported in this article are conducted with a computational domain that contains the geometrical features of the H6 thruster (Fig. 3). The H6 is a 6kW-class thruster developed in a joint effort of the University of Michigan, the Air Force Research Laboratory (AFRL) and the Jet Propulsion Laboratory (JPL) [28,29]. It features a centerline-mounted cathode and is designed for nominal operation at 300V, discharge current of 20A, and 20 mg/s flow rate. Under these conditions, 400mN of thrust and a specific impulse of approximately 1950s are achieved. This thruster was later modified for the proof-of-concept of magnetic shielding [32], a technique that reduces the channel erosion by orders of magnitude and enables the use of Hall thrusters for deep space missions [33]. The decision of using the H6US (for unshielded) for our Hall2De validation activities is motivated by the extensive range of measurements obtained in this original configuration compared to the magnetically shielded configuration (H6MS).

In order to investigate the consequences of extending the plume region contained in the computational domain, two different meshes are considered in our simulations. In the "short" domain, the magnetic field line that emanates at the outer radius of the keeper orifice ends at the right (z_{max}) boundary. In the "extended" domain, the z_{max} boundary is pushed to the right so the same magnetic field line now goes around to exit at the upper left boundary (Fig. 4). This modification has important implications in the electron motion. Approximately three quarters of the electrons generated at the cathode are employed for neutralizing the beam (i.e., at a 20A operating condition, the ion beam current is approximately 15A), while the remainder cross magnetic field lines to enter the acceleration channel.

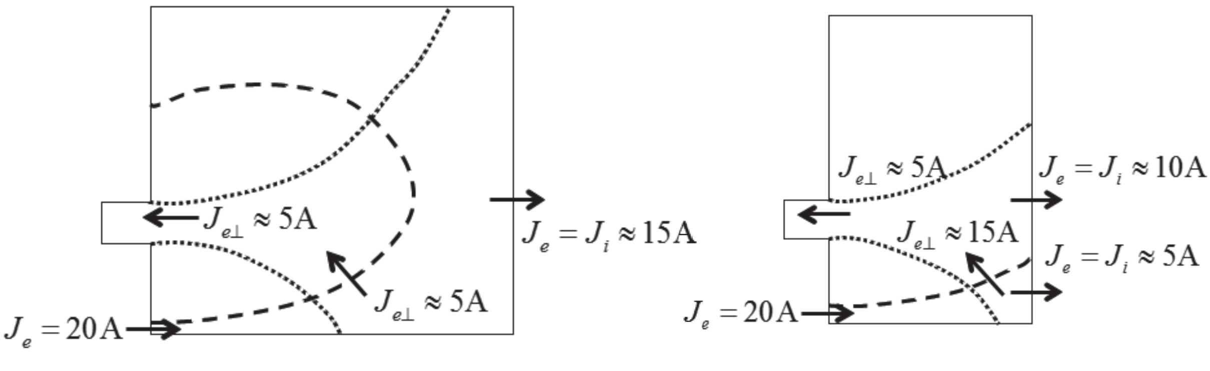

Fig. 4: Schematic of electron current transport across the magnetic field line emanating from the outer radius of the cathode exit (dashed line) in the extended (left) and short (right) computational domains with 20A operating condition. The ion beam is bounded by dotted lines. The subscript $\perp$ denotes transport perpendicular to magnetic field lines.

Neutralization of the beam is imposed at the outflow boundaries, z_{max} and r_{max}, by prescribing a condition for the electron current density to be equal to the ion current density at each edge. As shown in the schematic of Fig. 4, if the cathode B-line ends at the rightmost boundary (as in the case of the short domain), the boundary condition for beam neutralization forces neutralizing electrons to cross magnetic field lines. In the extended domain, neutralization of the beam does not require electrons moving across magnetic field lines, as the electrons find the path of least resistance to reach the z_{max} boundary in their motion along the B-lines that emanate from the keeper orifice of the hollow cathode. Only the electrons that are driven to the acceleration channel need to move perpendicularly to B-lines.

In the following sections, we show simulation results in the "short" and "extended" domain and comment on the differences observed due to the different distribution of electron current density in the cathode plume.

IV. The significance of anomalous transport of electrons across magnetic field lines in the ion beam

Previous work by Mikellides et al. [11] showed a 2-D distribution of anomalous collision frequency that allowed simulations to reproduce experimental measurements. This map was constructed by extension along magnetic field lines of a collision frequency profile defined along the centerline of the acceleration channel (Fig. 5) and has evolved as new experimental results have become available. We note that the anomalous collision frequency required outside the channel is several orders of magnitude higher than that predicted by classical mechanisms and comparable to the electron cyclotron frequency, resulting in an effective Hall parameter close to unity. It has been shown in [34] that fast scanning probes inside the acceleration channel are likely to perturb the plasma in this region, which adds uncertainty to the portion of the anomalous collision frequency profile for approximately $z/L<1$. For this reason, two different profiles inside the channel are shown in Fig. 5. We use "profile 1" for our discussion on the implementation of anomalous transport in the ion beam and cathode plume. At the end of this paper, it is shown that making use of "profile 2" does not modify the plasma conditions in the plume but can lead to significant differences in thruster performance.

In this section, we present the hypothesis that electron transport across magnetic field lines from the cathode plume to the acceleration channel occurs preferentially through the main beam of ions [35]. To this effect, numerical tests are conducted in which the anomalous contribution to the electron resistivity across B-lines is only added in regions where the current density of beam ions is sufficiently large. In Fig. 6, the resulting 2-D contour plots of the spatial distribution for the anomalous collision frequency are shown. It can be observed that only classical collisions are allowed in large regions of the computational domain, particularly in the vicinity of the poles. This plot also sketches the most probable electron path from the cathode to the acceleration channel. The electron current would first parallel the magnetic field lines in the cathode plume. As the cathode plume is intersected by the main beam,

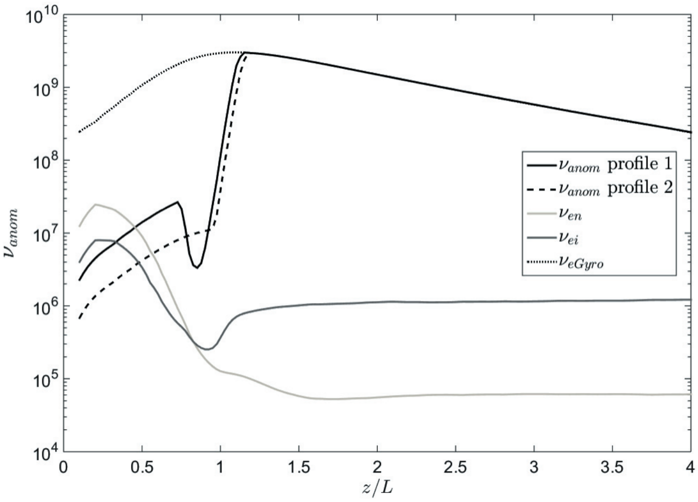

Fig. 5: Anomalous collision profiles along channel centerline. Two candidate profiles are shown. Profile 1 is used for comparisons between "short" and "extended" domain and at the end of this Section III a comparison of plasma properties and performance between the two is provided. Values of the electron-neutral (en), electron-ion(ei) and electron cyclotron frequencies (eGyro) are depicted for reference.

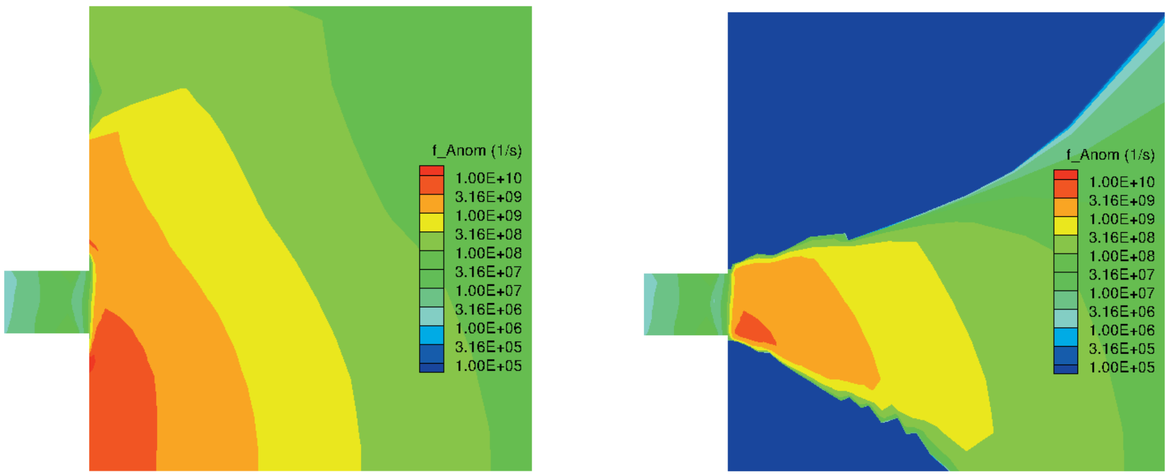

Fig. 6: 2-D contours of anomalous collision frequency in "short" domain. Left: anomalous collision frequency applied to the whole computational domain. Right: anomalous collision frequency applied to ion beam location.

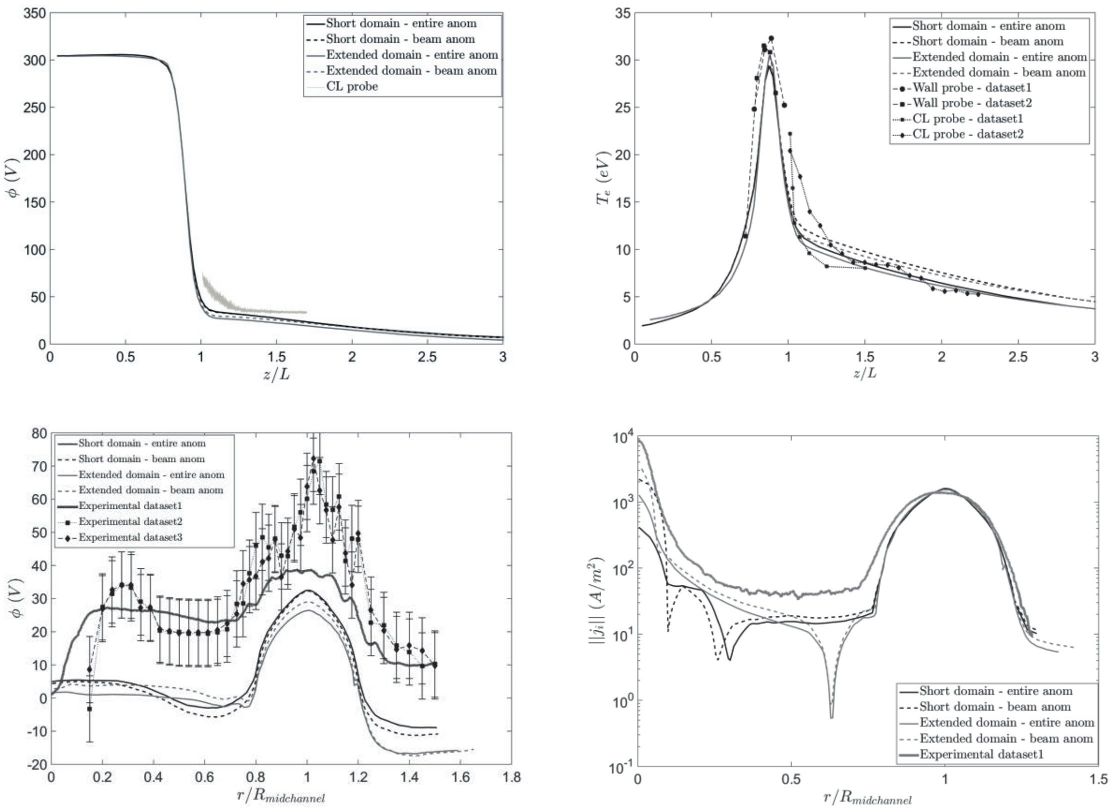

Fig. 7: Comparison between plasma parameters obtained from Hall2De simulations and experimental measurements. Two computational domains ("short" and "extended") and two anomalous collision frequency models ("entire anom": anomalous collision frequency applied in the whole computational domain, and "beam anom": anomalous collision frequency applied only where the current density of ions is large enough) are considered. First row: plasma potential, ϕ, and electron temperature, T_e, along channel centerline. Second row: plasma potential and total ion current density, $|j_i|$, along a radial profile located at z/L = 1.19. Dips in the ion current density are due to changes in the direction of the flow.

electrons can then easily move across magnetic field lines towards the acceleration channel due to the low Hall parameter produced by the addition of the anomalous collision frequency.

Figure 7 depicts the electron temperature and plasma potential along the channel centerline, and the plasma potential and ion current density along a radial profile located at z/L=1.19 for simulations run in the "short" and "extended" computational domains and with and without the cut-off in the anomalous collision frequency. All simulations were run with nominal vacuum chamber background pressure conditions of $1.4x10^{-5}$ Torr and two fluids for modeling the motion of high and low energy ions separately, with a threshold between populations set a 50V [30]. The IAT-driven anomalous collision frequency in the cathode plume has not been included in these simulations and will be the focus of the next section. Experimental measurements were obtained using wall probes and fast scanning injected probes. Temperature measurements at the channel walls have been extrapolated to the channel centerline assuming isothermal B-lines. Injected probes are known to perturb the plasma upstream of the peak magnetic field [34] and, in consequence, only measurements in the plume are shown. Radial profile data was obtained from [36] (dataset 1) and [37] (datasets 2 and 3). Table I summarizes performance variables for the four examined cases. Results show that plasma properties and performance are not significantly affected in this numerical experiment, suggesting that the discharge conditions are not sensitive to restricting the location of the anomalous collision frequency to regions of large ion current density. An additional hypothesis can be then made on anomalous transport being the product of collisionless wave growth mechanisms between ions and electrons. This is the subject of our companion paper [12], in which it is postulated that conditions for the growth of acoustic waves in the plasma exist in the acceleration region. The equations of motion for wave action also show that the waves are convected with the ion velocity into the plume. Even though is not shown here, increasing or reducing the threshold value of the ion current for cutting off the anomalous collision frequency does not have a significant effect on the discharge.

A more exhaustive investigation of the plasma profiles along the centerline reveals that small differences exist between the solution in the short and extended domains. In particular, the potential in the plume (Fig. 7, left) for the short domain is slightly higher (by approximately 5V) than in the extended domain. The use of Ohm's law (1) allows us to explain the different increase in the potential at the plume region with respect to the potential at the keeper exit (assumed here at 0V). The electric field integrated along the electron path determines the voltage differential with respect to the cathode and is proportional to both the resistivity and the electron current density. In the intersection of the beam with the cathode plume, the anomalous collision frequency reaches to the thruster centerline, facilitating the electron transport across B-lines (Fig. 6). Since the Hall parameter is approximately unity (Fig. 5), the resistivity is as low as it can possibly be. We can determine then that the resistivity is approximately equal in the short and extended domains. However, as shown in Fig. 4, the current density across magnetic field lines is higher in the short domain, which produces larger electric fields than in the extended domain, for the same resistivity. Thus, the difference in current density across magnetic field lines between the short and extended domain results in the small ~5V difference in the plume potential along the channel centerline.

	Short domain		**Extended domain**		**Experimental**
	Entire anom	**Beam anom**	**Entire anom**	**Beam anom**	
Discharge current (A)	20.03	20.04	20.06	19.98	20.00
Thrust (mN)	330.2	330.2	334.8	334.7	401.0
Beam current (A)	14.26	14.29	14.19	14.98	16.70
Fraction of Xe+	0.836	0.831	0.828	0.827	0.755
Fraction of Xe++	0.155	0.160	0.163	0.164	0.161
Fraction of Xe+++	0.009	0.009	0.009	0.009	0.084
Mass efficiency	0.933	0.931	0.901	0.952	0.995
Current efficiency	0.986	0.986	0.986	0.986	0.973
Charge efficiency	0.713	0.713	0.710	0.750	0.835
Anode efficiency	0.473	0.472	0.475	0.474	0.682

Table I: Performance parameters for four simulation cases of the "short" and "extended" computational domain, using the anomalous collision frequency "profile 1" (Fig. 5) extended to the entire computational domain ("entire anom") and cut off in regions of low ion current density ("beam anom"). Experimental measurements [38] are also provided for comparison.

V. Anomalous collision frequency in the cathode plume

The most important difference between the experimental and simulation results in Fig. 7 is found for the radial profile of the plasma potential. The measured ~25V gradient in the plasma potential close to the cathode and the plateau between the cathode plume and the beam are not captured in Hall2De simulations. Being able to replicate this feature is of key importance at the time of, for instance, assessing pole erosion since the difference between the plasma potential at some distance from the pole wall and the potential at which the pole face is set will determine a significant fraction of the energy of ions impacting the pole surface. To achieve a close agreement with experiments, it is necessary to increase the resistivity in the cathode region in a way such that the plasma potential is forced to rise for enabling the electron current required in the discharge. A decade-long numerical and experimental study of hollow cathodes at JPL [18-24] has demonstrated the existence and measured the power spectra of ion-acoustic turbulence downstream of the cathode exit. This turbulence manifests in the hydrodynamic equations as an anomalous collision frequency term, which increases resistivity in the direction parallel to the magnetic field and reduces it in the perpendicular direction whenever the Hall parameter is large. In fact, in the OrCa2D simulations [24], the addition of Sagdeev's model (3), which is an over-simplified expression that assumes saturation of the instability growth, allowed for simulation results that showed good agreement with measured discharge current and voltage in cathode tests. The presence of IAT-driven anomalous resistivity has also been confirmed by recent measurements [22].

A. Plasma parameters in the presence of anomalous collision frequency in the cathode plume

Figure 8 presents the effect of including the cathode anomalous frequency in our Hall2De simulations. The free parameter, K, in Eq. (3) has been chosen in a way such that the simulation in the extended domain closely reproduces the measured gradient of the plasma potential. The value of the coefficient is the same for all simulations

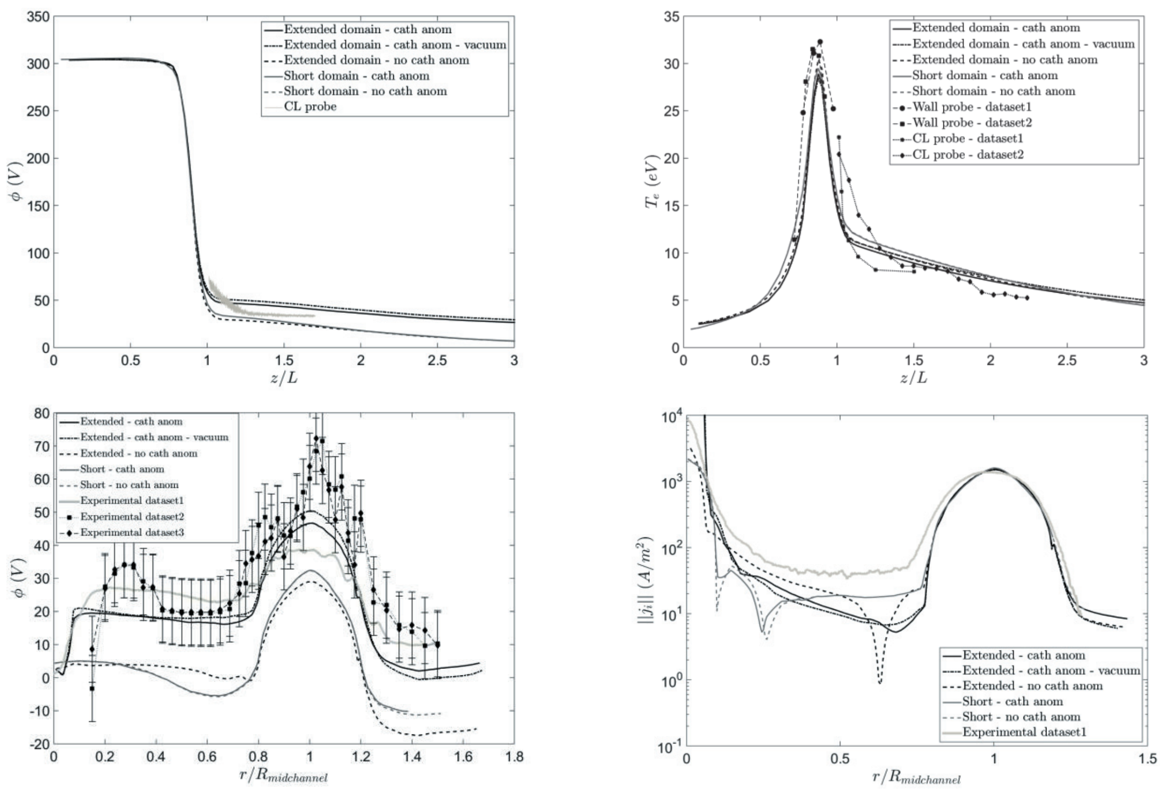

Fig. 8: Comparison between plasma parameters obtained from Hall2De simulations with and without the inclusion of the cathode anomalous collision frequency in the short and extended domains, and experimental measurements. First row: plasma potential, ϕ, and electron temperature, T_e, along channel centerline. Second row: plasma potential and total ion current density, $|j_i|$, along a radial profile located at z/L = 1.19

and found to be consistent to the typical values found in our cathode simulations with OrCa2D [24]. The radial profile for the simulation in the extended domain closely resembles the experimental values. In the short domain, the gradient in the potential between the cathode plume and the inner pole region is not captured. Further explanation of this phenomenon will be given in the next subsection. Attending at the radial profile at z/L=1.19 for the extended domain, it can be observed that the main effect of the inception of the plasma potential gradient is a shift in the entire profile up to higher values. With respect to the ion current density, the new distribution of the plasma potential clearly modifies the ion velocity field, as no dips (indicative of changes in velocity direction) are observed. This can be attributed to low-energy plume ions being turned towards the wall and the cathode region due to the voltage differentials. However, the average ion current density (without taking the dips into consideration) remains similar for all the cases examined. We have also included a simulation at vacuum conditions to stress that the new features observed in the plasma parameters in the presence of cathode anomalous collision frequency are independent of the background pressure. As the axial profiles show, the location of the acceleration region and the peak of the electron temperature are not affected by changes in the plasma properties in the plume.

B. Physical explanation of the existence of the plasma potential gradient in the cathode region

The approach presented here is not our first attempt at explaining the physics behind the measured features of the plasma potential in the plume. In [30], the gradient was captured in the simulations by assuming that the anomalous collision frequency across magnetic field lines was zero for the entire cathode plume. Enforcing this condition led to large electric field values at the magnetic field lines for which the anomalous collision frequency had been cut-off in order to drive electrons from the cathode plume into the acceleration channel. This approach exhibited several weaknesses. The plasma density in the region where the anomalous collision frequency was set to zero was not large enough to explain damping of the collisionless mechanisms that contribute to the anomalous transport. The results were also highly dependent on the background conditions. In effect, most of the electron transport occurred at the intersection of the main beam with the cathode plume. In this region, the plasma density is largely affected by the presence of background neutrals. As the anomalous collision frequency was set to zero, classical collisions dominated, with a resulting resistivity depending on the plasma density as $\sim 1/n_e^2$. Thus, the resistivity was larger in vacuum conditions to the extent that the radial gradient in the potential was observed in numerical simulations with assumed vacuum but not in simulations run with typical vacuum chamber conditions. Finally, plasma properties along the cathode centerline extracted from the simulations did not agree well with experimental measurements.

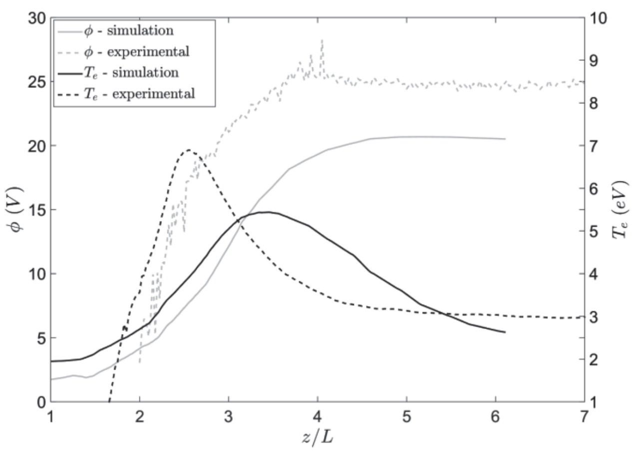

Fig. 9: Comparison between plasma parameters (plasma potential and electron temperature) along the thruster centerline obtained from Hall2De simulations with cathode anomalous collision frequency in the extended domain, and experimental measurements. Results agree qualitatively as the model for anomalous collision frequency in the cathode plume (3) is simplistic and the grid resolution is not fine enough to capture plasma properties in detail.

The physical mechanism that allows for the formation of the plasma potential gradient in the presence of IAT-driven anomalous collision frequency in the cathode is as follows. At the cathode exit, classical collisions are dominant, leading to an increase in the potential. This can be observed in Fig. 9 where the first recorded value of the potential is above the boundary condition, set at 0V. In the absence of any anomalous mechanism, the resistive term in Ohm's law (1) parallel to magnetic field lines is rapidly overcome by the pressure term. As the plasma density decreases axially, the pressure term acts towards decreasing the value of the potential. This can be observed in Fig. 10 (top-right) for the short domain. If sufficient anomalous collision frequency is added to the resistive term, the potential never decreases in the axial direction (Fig. 10 (top-left)). Having an axial increase in the potential is not a sufficient condition for explaining the features observed in the radial profile of the plasma potential as the cathode ions would tend to expand in the radial direction if a "potential barrier" is set in the axial direction. However, the Hall parameter is very large in the radial direction due to the steep decrease in the density and the absence of anomalous collision frequency across magnetic field lines. We argue that the two conditions, positive plasma gradients axially and large Hall parameters radially, results in the formation of the radial and axial gradient of the potential observed in numerical simulations (Fig. 10) and probe measurements (Figs. 8,9). The plasma density in the

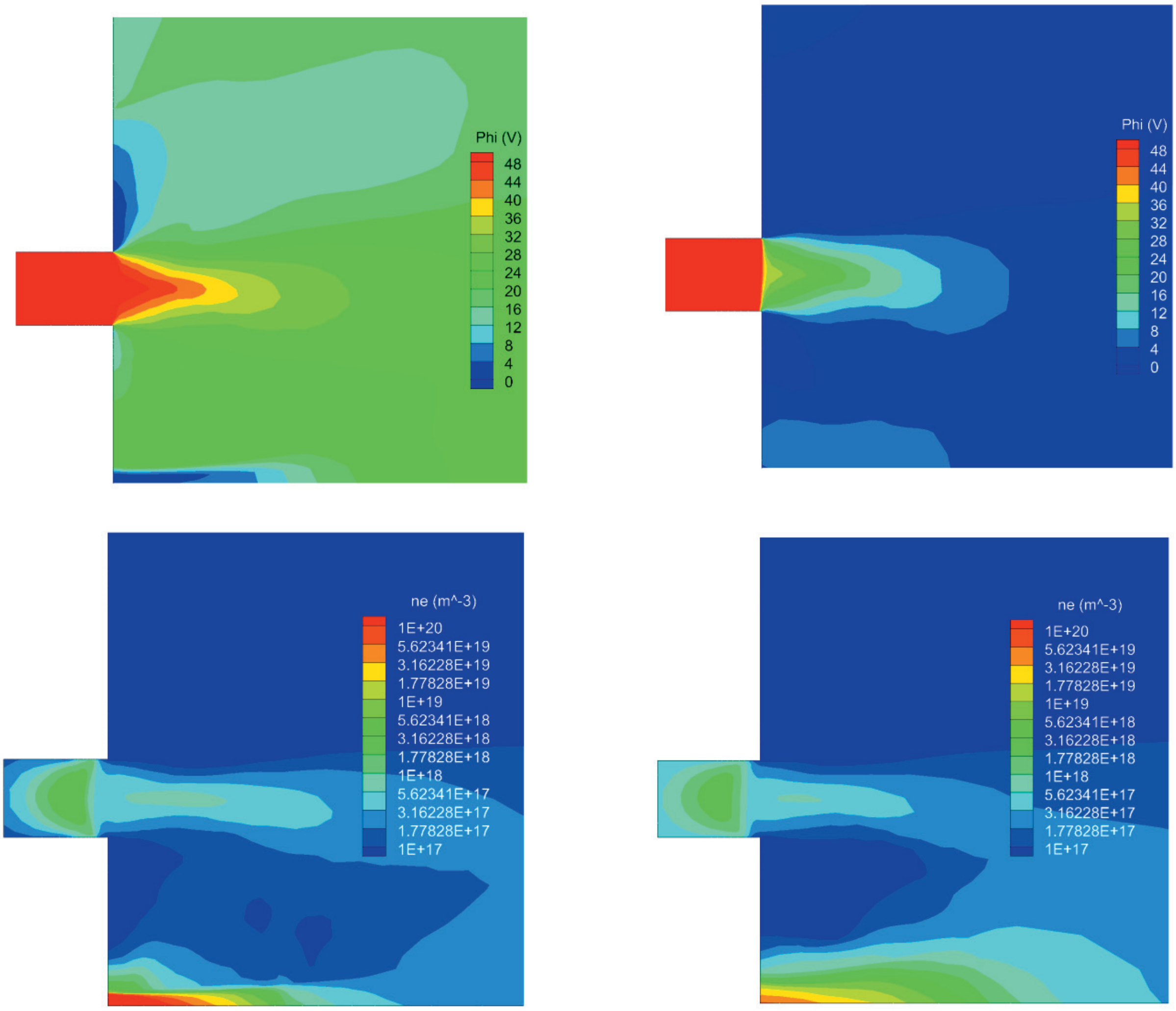

Fig. 10: Time-averaged plasma potential contours scaled at 48V (top) and plasma density contours (bottom) for extended domain (left) and short domain (right) when cathode anomalous collision frequency is included (same value of K in Eq. (3) in both cases). Only the extended domain shows a gradient in the plasma potential as more electron current flows in the z-direction, increasing the potential gradient for the same value of the resistivity.

cathode plume remains consequently confined by the axial and radial gradients in the potential, as observed in Fig. 10 (bottom-left). It is important to note that if we had not restricted the presence of anomalous collision frequency across B-lines to the ion beam in Section IV, the resistivity across magnetic field lines in the vicinity of the cathode exit would have been low and the cathode ions would have expanded in the radial direction, impeding the formation of the potential gradient. In the short domain, the electrons are required to move across magnetic field lines to neutralize the beam, which results in lower values of the electron current density along B-lines (as the same current is spread over a larger section). Thus, the presence of cathode anomalous collision frequency is not as effective for two reasons: the ratio between the electron drift velocity and the thermal velocity decreases in Eq. (3) and the current density decreases in Eq. (1). We have attempted to increase the coefficient K in the short domain simulations to obtain plasma contours in agreement with the experimental measurements in the short domain with no success. The latter stresses the importance of selecting an appropriate computational domain such that boundary conditions do not perturb the plasma properties.

In Fig. 9, we show the comparison between experimental measurements in [37] along the thruster centerline and numerical simulations in the extended domain. Even though the location of the plasma potential and electron temperature gradients are not matched perfectly, probably due to an over-simplistic model for the cathode anomalous collision frequency (3), we can capture qualitatively the measured behavior of the plasma in the cathode plume. This piece of experimental evidence reinforces our assumption that the existence of anomalous transport mechanisms in the cathode plume is responsible for the plasma potential gradients observed in the radial direction at the boundary of the cathode plume.

We also need to question the sensitivity of these results on grid resolution. In the computational domains used in these simulations, the keeper exit is captured within one boundary edge. This implies that the radial gradient of the plasma potential shown in Fig. 10 occurs from the first row of cells (counting from the thruster centerline) to the second. The plasma density is also confined in the first row of cells due to the axial and radial gradients in the plasma potential than do not allow for the expansion of ions (except when oscillations occur, which will be

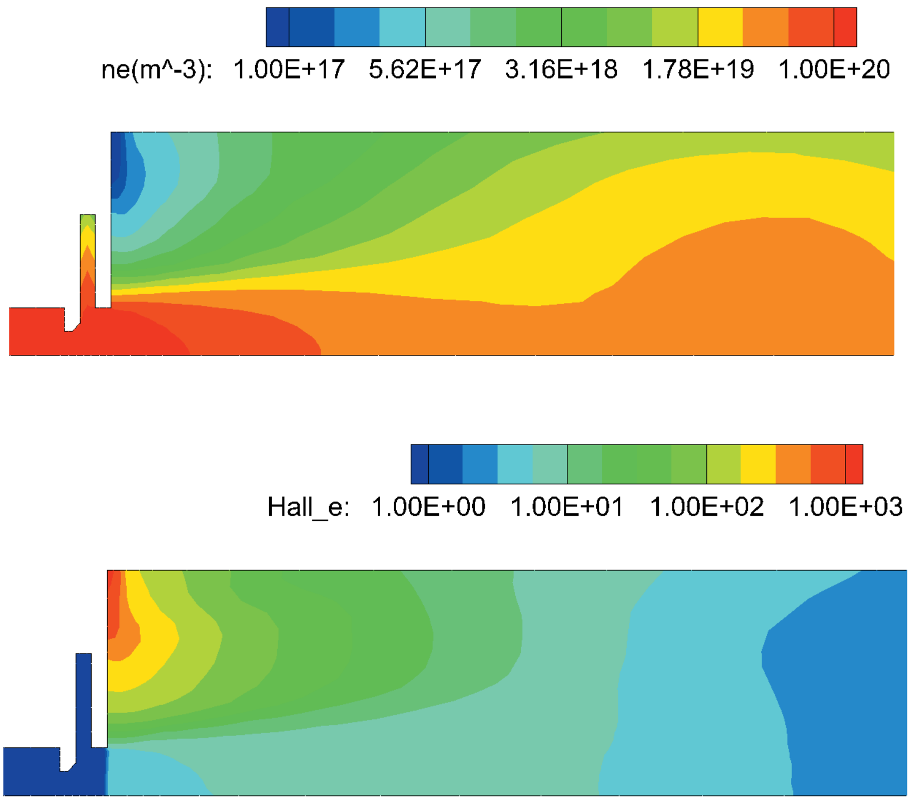

Fig. 11: Plasma density and Hall parameter, Ω_e, in the cathode plume in an OrCa2D simulation of a LaB6 cathode operating at 100A in the presence of a magnetic field similar in topology to that of the H6US

discussed in the next subsection). The fact that steep changes in the plasma density and potential occur within two rows of cells warrants further investigation with refined computational grids in the cathode region. Simulations with a refined computational domain are not currently available but will be the subject of a near-term computational campaign. However, some insight on the plasma properties at the keeper exit with a refined grid can be obtained from OrCa2D simulations [24] of the cathode discharge in the presence of a magnetic field, where sufficient resolution is indeed employed in the vicinity of the keeper orifice. The available simulations at this time cannot offer a direct comparison with Hall2De results for two reasons: the operating conditions do not exactly match those in the Hall2De simulations and the location of the anode in OrCa2D has an effect on the plasma distribution in the cathode plume. Nonetheless, characteristic features of the cathode plume in Hall2De simulations can also be observed in the OrCa2D contour plots shown in Fig. 11. The bulk of the plasma remains confined by the magnetic field line that intersects the edge of the keeper exit. The plasma density decreases by two orders of magnitude in a distance comparable to the radius of the keeper exit in the radial direction and, in consequence, the Hall parameter also decreases steeply in the same direction.

C. Low-frequency plasma oscillations

An additional consequence of the inclusion of the IAT-driven anomalous transport in the cathode is the recovery of discharge oscillations that are in the frequency range of the breathing mode experimentally observed in the H6 thruster. Fig. 12 shows the evolution in time of the discharge current and thrust in the short and extended domains, when the anomalous collision frequency model (3) for the cathode plume has been included in the simulations. A fast Fourier transform (FFT) analysis of the time-resolved discharge current in the extended domain reveals a peak at 18 kHz masked with noise in the 10 to 40 kHz range. Root mean square (RMS) oscillation amplitude is 6%. The observed behavior is consistent with experimental measurements [38]. The physical mechanism behind these oscillations is mainly cathode-driven and can be best understood by looking at the time evolution plot depicted in Fig. 13. First, plasma density builds up at the cathode exit (dashed grey line in Fig. 13). These ions cannot move away from the cathode plume due to the plasma potential gradients opposing their motion. As the density of ion builds due to ionization, the ion pressure overcomes the potential barrier and ions are allowed to move radially and axially. This phenomenon can be observed in peaks in the continuous grey line (density at a radial location a few millimeters away from the cathode plume) corresponding to dips in the dashed grey line in Fig. 13. When ions are allowed to escape from the cathode plume region, the resistivity (and with it the plasma potential) decreases at the boundaries of the cathode plume. After the expansion, as the cathode plume region is progressively replenished of ions due to the cathode inflow and ionization, the anomalous collision frequency and the Hall parameter rise. This phenomenon leads to increased resistivity and the inception of the gradient in the plasma potential in both axial and radial directions. At this point, the cycle restarts, with ionization rates being enhanced by the confinement of the plasma.

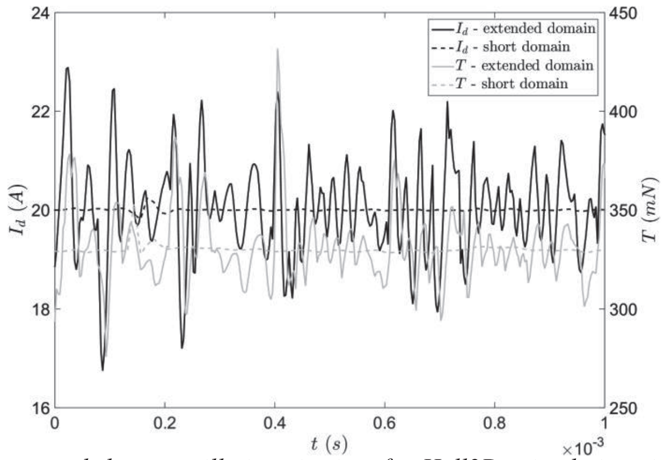

Fig. 12: Discharge current and thrust oscillations in time for Hall2De simulations in the short and extended domain with cathode anomalous collision frequency included.

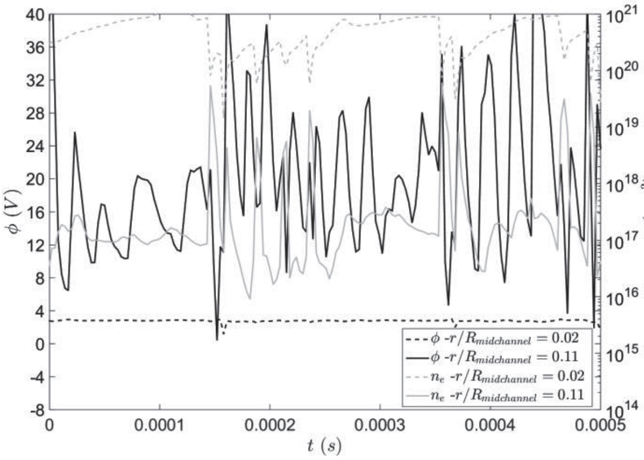

Fig. 13: Time diagram depicting oscillations of the plasma potential and density in "numerical probes" collocated at the keeper exit plane and different radial locations. Inside the cathode plume ($r/R_{midchannel}$=0.02), no oscillations in the potential are recorded. Outside, plasma potential oscillations exist. As the density inside the cathode plume increases, the resistivity decays, which results in lower plasma potentials with respect to the cathode potential. Ion particles can then move radially as the potential barrier disappears, which translates in peaks in the plasma density at $r/R_{midchannel}$=0.11 when the density at $r/R_{midchannel}$=0.11 reaches a minimum.

The noise observed in time dependent plots (Figs. 12 and 13) can be a consequence of the different ionization rates of singly, doubly and triply charged ions since all contribute to the plasma density build-up. There may be also a numerical contribution related to the lack of resolution in the region of interest. The computational simulations in a refined grid outlined in the previous section will also be used to determine with higher fidelity the behavior of the plasma properties during these low-frequency oscillations.

D. Effect of changes in the anomalous collision frequency profile inside the channel

We conclude this section with a comparison of the results of numerical simulations run with profiles 1 and 2 in Fig. 5. Even though the profile employed in the previous investigations ("profile 1") matches relatively well the experimental measurements, we observe that the predicted peak electron temperature is approximately 5eV lower than measured, with a shape that is narrower than what experiments predict. We attempt to obtain a bound for our uncertainty regarding the plasma conditions inside the channel by using a profile that yields lower values of the anomalous collision frequency in this region, as this modification typically results in a wider electron temperature peak [39]. Fig. 14 shows the plasma parameters obtained with the two profiles. The first observation to be made is that the radial profiles of the plasma potential and ion current density in the plume (z/L=1.19) are not significantly modified, which suggests that the discussion of previous sections is valid regardless of the plasma conditions inside the acceleration channel. Examination of the centerline profiles upstream of the plume region reveals that modifying the anomalous profile inside the channel leads to an electron temperature distribution that in fact is wider and with a peak value in agreement with the experimental data from wall probes. However, the temperature in the ionization region upstream of the channel is likely larger than what wall probe measurements suggest. The plasma potential is also modified in a way such that it is smoothed out upstream.

Table II summarizes performance predictions for the two profiles. We observe that "profile 2" is a configuration that produces higher thrust with the same discharge current. Whilst the thrust value predicted by "profile 1" under-predicts the experimental measurements by 18%, the disagreement in thrust is reduced between simulations and experiments to values below 7% with "profile 2". The reason behind this difference in performance is related to the higher electron temperature upstream of the channel, which produces enhanced ionization and also a higher fraction of doubly and triply charged ions. In fact, "profile 1" over-predicts the fraction of singly charged ions, which also results in lower values of the beam current. "Profile 2" produces results that agree well with experiments both in terms of ion beam current and fraction of singly charged ions. We note that the fraction of triply charged ions is under-predicted for both profiles. The reason for this phenomenon is unknown at the moment since an analysis of the cross sections used in our model [40-42] does suggest that the measured fraction of triply charged ions is not

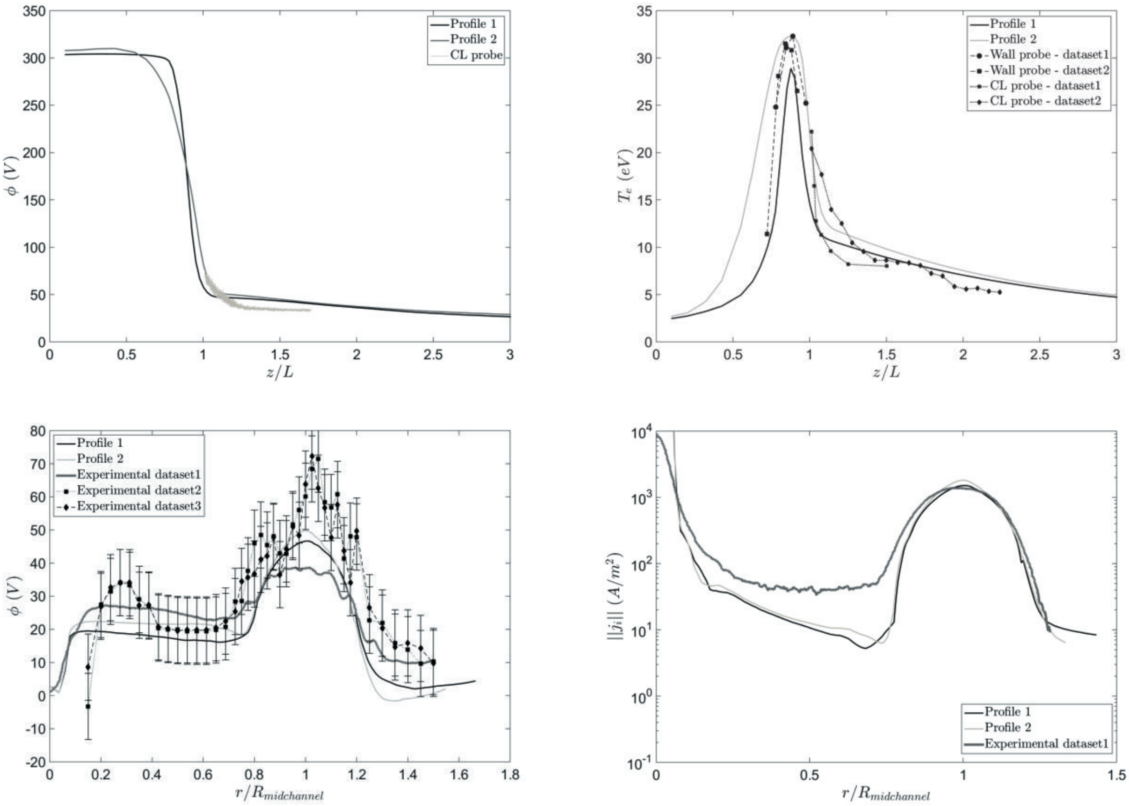

Fig. 14: Comparison between plasma parameters obtained from Hall2De simulations with cathode anomalous collision frequency in the extended domain for anomalous collision frequency profiles 1 and 2 (Fig.5) and experimental measurements. First row: plasma potential, ϕ, and electron temperature, T_e, along channel centerline. Second row: plasma potential and total ion current density, $|j_i|$, along a radial profile located at z/L = 1.19

possible provided the plasma conditions in the thruster. The existence of metastable states that require less energy for ionization can be a possible cause for this phenomenon that will be investigated in the future. Mass efficiency is higher than unity in "profile 2" as this variable is computed based on the anode mass flow rate and does not include the cathode flow rate or the presence of background neutrals.

Since no temperature or plasma measurements are available in the first one-third of the acceleration channel, we cannot make a definite claim on the prevalence of one of the profiles versus the other at this moment. Future measurements using laser-induced fluorescence (LIF) or the development of a phenomenological model for the anomalous transport may help determining the conditions of the plasma upstream of the channel. However, by examining the plasma conditions in the plume, we have shown that our efforts to include in the numerical simulations a realistic picture of the electron transport in the plume is independent of our uncertainty with respect to the plasma conditions inside the channel.

	Profile 1	Profile 2	Experimental
Discharge current (A)	19.96	20.06	20.00
Thrust (mN)	328.7	374.1	401.0
Beam current (A)	15.12	16.92	16.70
Fraction of Xe+	0.827	0.749	0.755
Fraction of Xe++	0.164	0.228	0.161
Fraction of Xe+++	0.009	0.024	0.084
Mass efficiency	0.960	1.024	0.995
Current efficiency	0.757	0.843	0.973
Charge efficiency	0.986	0.979	0.835
Anode efficiency	0.458	0.600	0.682

Table II: Performance parameters obtained from Hall2De simulations in the extended domain and different anomalous collision profiles (see Fig. 5). Experimental values are provided for comparison.

VI. Conclusion

We showed in this paper the importance of an accurate modeling of the plasma conditions in the plume region of Hall-effect thrusters for the validation of the numerical code Hall2De against experimental measurements. Hall2De simulations include the physical location of the cathode orifice, allowing for the transport of electrons to the acceleration channel and for beam neutralization to be fully captured in the computational domain.

We first commented on the requirement of constructing a computational domain sufficiently large. Neutralizing electrons are artificially forced to cross magnetic field lines in computational domains where the magnetic field lines that intersect the cathode exit also intersect the outflow boundary of the domain. By extending the computational domain in the axial direction in a way such that the cathode B-lines do not cross the outflow boundary, the electrons are able to neutralize the entire beam describing paths parallel to the field lines, with less resistivity than the motion across B-lines. Thus, it was shown that the boundary conditions can interfere with the distribution of electron current densities in the plume and that some initial thought is necessary at the time of defining a computational domain that produces numerical results that are not negatively influenced in their accuracy by the boundary conditions.

We also showed by numerical simulation that the anomalous collision frequency required to move electrons across magnetic field lines in the near plume towards the acceleration channel can be set to zero anywhere in the computational domain except in the ion beam, without altering the plasma solution or the performance values. This finding is in agreement with our previous arguments that the path of least resistance for the electrons to reach the acceleration channel is through the ion beam [35], and strengthens the hypothesis, presented in [12], that the motion of ions plays a critical role in the convection of the collisionless mechanisms that result in enhanced mobility of electrons.

Finally, we demonstrated the significance of accounting for IAT-driven anomalous collision frequency in the near-cathode regions by including a simplified model based on Sagdeev's formulation (3) in Hall2De simulations. This new model actually leads to an increase of the resistivity of electrons parallel to magnetic field lines. Due to the implementation of this model, the measured radial and axial profiles of the plasma potential in the near plume and thruster centerline, respectively, were reproduced with high fidelity by the simulations. It was also shown that, when a short computational domain that disturbs electron transport is employed, the features of the measured radial profile, especially the value of the potential plateau in the vicinity of the inner pole and the gradient between this value and the cathode potential, cannot be captured due to the decreasing electron current density parallel to B-lines. Plasma properties obtained while varying the assumed background pressure in the simulations exhibited very small changes.

We finished this discussion on the modeling of plasma properties in the plume by showing that uncertainties in the plasma measurements inside the acceleration channel, which were bounded with two different distributions of the anomalous collision frequency in our simulations, do not significantly affect the plasma conditions and electron transport in the near plume.

Acknowledgments

The research described in this paper was carried out by the Jet Propulsion Laboratory, California Institute of Technology, under a contract with the National Aeronautics and Space Administration. The support of NASA's Space Technology Mission Directorate through the Solar Electric Propulsion Technology Demonstration Mission (SEP TDM) project is gratefully acknowledged. The authors wish to acknowledge Dr. Ira Katz for the useful comments and discussions on the content of this manuscript.

References

[1] M. Hirakawa and Y. Arakawa, "Numerical simulation of plasma particle behavior in a Hall thruster", AIAA paper 96-3195, in proceedings of the 32nd AIAA Joint Propulsion Conference, Lake Buena Vista, Florida, 1996, p. 3195

[2] J. C. Adam, A. Heron and G. Laval, "Study of stationary plasma thrusters using two-dimensional fully kinetic simulations", Physics of Plasmas, Vol. 11, 2004, 295.

[3] J. J. Szabo, "Fully kinetic numerical modeling of a plasma thruster", Ph.D. thesis, Massachusetts Institute of Technology, 2001.

[4] J. M. Fife, Ph.D. thesis, Massachusetts Institute of Technology, 1998.

[5] Parra, E. Ahedo, J. M. Fife, and M. Martinez-Sanchez, "A two-dimensional hybrid model of the Hall thruster discharge", Journal of Applied Physics, Vol. 100, 2006, p. 023304.

[6] M. Fife, M. Martinez-Sanchez, and J. Szabo, "A numerical study of low-frequency discharge oscillations in Hall thrusters", AIAA paper 1997-3052, in proceedings of the 33rd AIAA Joint Propulsion Conference, Seattle, WA, 1997.

[7] P. Boeuf and L. Garrigues, "Low Frequency Oscillations in a Stationary Plasma Thruster," Journal of Applied Physics, Vol. 84, 1998, p. 3541.

[8] S. Barral and E. Ahedo, "Low-frequency model of breathing oscillations in Hall discharges", Physical Review E, Vol. 79, 2009, p. 046401.

[9] I. G. Mikellides and I. Katz, "Numerical simulations of Hall-effect plasma accelerators on a magnetic-field-aligned mesh", Physical Review E, Vol. 86, 2012, p. 046703.

[10] J. Bohm, E. Burhop, and H. Massey, "Characteristics of electrical discharges in magnetic fields", in National Nuclear Energy Series, Manhattan Project Technical Section, Division I, Guthrie, A. and Waterling, R. K., Eds., McGraw-Hill, New York, 1949.

[11] I. G. Mikellides, I. Katz, and R. R. Hofer, "Design of a laboratory Hall thruster with magnetically shielded channel walls, phase I: numerical simulations", AIAA paper 2011-5809, in proceedings of the 47th AIAA Joint Propulsion Conference, San Diego, California, 2011.

[12] I. Katz, I. G. Mikellides, B. A. Jorns and A. Lopez Ortega, "Hall2De simulations with an anomalous transport model based on the electron cyclotron drift instability", IEPC paper 2015-402, in Proceedings of the 34th International Electric Propulsion Conference, Kobe, Japan, 2015.

[13] D. W. Forslund, R. L. Morse, and C. W. Nielson, "Electron Cyclotron Drift Instability", Physical Review Letters, Vol. 25, 1970, p. 1226

[14] P. Coche and L. Garrigues, "A two-dimensional (azimuthal-axial) particle-in-cell model of a Hall thruster", Physics of Plasmas, Vol. 21, 2014, 023503

[15] A. Ducrocq, J. C. Adam, A. Heron, and G. Laval, "High-frequency electron drift instability in the cross-field configuration of Hall thrusters," Physics of Plasmas, Vol. 13, 2006, 102111.

[16] S. Tsikata, N. Lemoine, V. Pisarev, and D. M. Gresillon, "Dispersion relation of electron density fluctuations in a Hall thruster plasma, observed by collective light scattering," Physics of Plasmas Vol. 16, 2009, 033506.

[17] J. Cavalier, N. Lemoine, G. Bonhomme, S. Tsikata, C. Honore, and D. Gresillon, "Hall thruster plasma fluctuations identified as the ExB electron drift instability: Modeling and fitting on experimental data", Physics of Plasmas Vol. 20, 2013, 082107.

[18] D. M. Goebel, K. K. Jameson, I. Katz and I. G. Mikellides, "Energetic ion production and electrode erosion in hollow cathode discharges", IEPC paper 05-269, in Proceedings of the 29th International Electric Propulsion Conference, Princeton, New Jersey, 2005.

[19] I. G. Mikellides, I. Katz, D. M. Goebel, J. E. Polk, and K. K. Jameson, "Evidence of non-classical plasma transport in hollow cathodes for electric propulsion", Journal of Applied Physics, Vol. 101, No. 6, 2007, 063301

[20] I. G. Mikellides and I. Katz, "Wear mechanisms in electron sources for ion propulsion I: neutralizer hollow cathode", Journal of Propulsion and Power, Vol. 24, No. 4, 2008, 855-865

[21] I. G. Mikellides, I. Katz, D. M. Goebel, K. K. Jameson and J. E. Polk, "Wear mechanisms in electron sources for ion propulsion II: discharge hollow cathodes", Journal of Propulsion of Power, Vol. 24, No 4, 2008, 866-879

[22] B. A. Jorns, I. G. Mikellides, and D. M. Goebel, "Ion acoustic turbulence in a 100-A LaB6 hollow cathode", Physical Review E, Vol. 90, 2014, 063106.

[23] B.A. Jorns, I.G. Mikellides and D.M. Goebel, "Temproal fluctuations in a 100-A LaB6 hollow cathode", IEPC Paper 2013-385, in Proceedings of the 33rd International Electric Propulsion Conference, Washington, DC, 2013

[24] I. G. Mikellides, D. M. Goebel, B. A. Jorns, J. E. Polk, and P. Guerrero, "Numerical simulations of the partially-ionized gas in a 100-A LaB6 hollow cathode", IEEE Transactions on Plasma Science, Special Issue on Plasma Propulsion, Vol. 43, No. 1, 2015, pp. 173-184.

[25] R. Marchand and M. Dumberry, "CARRE: a quasi-orthogonal mesh generator for 2D edge plasma modelling", Computer Physics Communications, Vol. 96, 1996, pp. 232-246.

[26] Z. Lin, T. S. Hahm, W. W. Lee, W. M. Tang, and R. B. White, "Turbulent Transport Reduction by Zonal Flows: Massively Parallel Simulations," Science, Vol. 281, 1998, pp. 1835-1837.

[27] I. Katz and I. G. Mikellides, "Neutral gas free molecular flow algorithm including ionization and walls for use in plasma simulations", Journal of Computational Physics, Vol. 230, 2011, pp. 1454-1464

[28] B. M. Reid, "The Influence of Neutral Flow Rate in the Operation of Hall Thrusters," Ph.D. Thesis, Aerospace Engineering, University of Michigan, 2009.

[29] D. L. Brown, C. W. Larson, J. M. Haas, and A. D. Gallimore, "Analytical extraction of plasma properties using a Hall thruster efficiency architecture", IEPC paper 2007-188, in proceedings of the 30th International Electric Propulsion Conference, Florence, Italy, 2007.

[30] A. Lopez Ortega and I. G. Mikellides, "A new cell-centered implicit numerical scheme for ions in the 2-D axisymmetric code Hall2De", AIAA paper 2014-3621, in proceedings of the 50th AIAA Joint Propulsion Conference, Cleveland, OH, 2014.

[31] R.Z. Sagdeev, A. Galeev, Nonlinear plasma theory, W. A. Benjamin, New York, 1969.

[32] I. G. Mikellides, I. Katz, R. R. Hofer, D. M. Goebel, K. H. de Grys and A. Mathers, "Magnetic shielding of the channel walls in a Hall plasma accelerator," *Physics of Plasmas,* vol. 18, no. 3, pp. 033501, Mar, 2011.

[33] J. R. Brophy, and L. Friedman, "Returning an Entire Near-Earth Asteroid in Support of Human Exploration Beyond Low-Earth Orbit," in IAF Global Exploration Conference, Washington, D. C., 2012.

[34] B. A. Jorns, R. R. Hofer, and D. M. Goebel, "Study of Probe Perturbation Effects in the H6US", Jet Propulsion Laboratory, California Institute of Technology, 2014, p. 52

[35] I. G. Mikellides, I. Katz, R. R. Hofer, and D. M. Goebel, "Hall-effect thruster simulations with 2-D electron transport and hydrodynamic ions", IEPC paper 2009-114, in Proceedings of the 31st International Electric Propulsion Conference, Ann Arbor, Michigan, 2009.

[36] K. K. Jameson, "Investigation of hollow cathode effects on total thruster efficiency in a 6 kW Hall thruster," Ph.D. thesis, UCLA, 2008

[37] M. Sekerak, "Plasma oscillations and operational modes in Hall effect thrusters", Ph.D. thesis, University of Michigan, 2014

[38] R. R. Hofer, D. M. Goebel, I. G. Mikellides, and I. Katz, "Design of a laboratory Hall thruster with magnetically shielded channel walls, phase II: experiments", AIAA paper 2012-3788, in proceedings of the 48th AIAA Joint Propulsion Conference, Atlanta, Georgia, 2012.

[39] I. G. Mikellides, A. Lopez Ortega, and B. Jorns, "The sensitivity of the acceleration zone on the anomalous collision frequency and implications on erosion predictions in simulations of magnetically shielded Hall thrusters", AIAA paper 2014-3897, in proceedings of the 50th AIAA Joint Propulsion Conference, Cleveland, Ohio, 2014.

[40] R. Rejoub, B. G. Lindsay, and R. F. Stebbings, "Determination of the absolute partial and total cross sections for electron-impact ionization of the rare gases", Physical Review A, Vol. 65, 2002, pp. 042713.

[41] W. Bell, N. Djuric, and G. H. Dunn, "Electron –impact ionization of In^+ and Xe^+", Physical Review A, Vol. 48, 1993, pp. 4286.

[42] I. Borovik, J. Rausch, J. Rudolph, M. Gharaibeh, S. Schippers and A. Muller, "Electron impact ionization of Xenon ions", Journal of Physics: Conference Series, Vol. 194, Part 6, 2009, pp, 062014.